

High-Sensitivity Imaging and Modeling of Ultra-Weak Photon Emission in Plants Under Stress

Yan-Xia Liu¹, Hai-Yu Fan¹, Yu-Hao Wang¹, Yan-Liang Wang², Sheng-Wen Li^{1,*}, Shi-Jian Li³, Xu-Ri Yao^{1,*}, Qing Zhao^{1,*}

¹*Center for Quantum Technology Research, School of Physics, Beijing Institute of Technology, Beijing 100081, China*

²*The Germplasm Bank of Wild Species & Yunnan Key Laboratory for Fungal Diversity and Green Development, Kunming Institute of*

Botany, Chinese Academy of Sciences, Kunming, Yunnan 650201, China

³*School of Integrated Circuits and Electronics, Beijing Institute of Technology, 100081 Beijing, China*

**Author for correspondence: lishengwen@bit.edu.cn (Sheng-Wen Li), yaoxuri@bit.edu.cn (Xu-Ri Yao), qzhaoyuping@bit.edu.cn (Qing*

Zhao)

Short title: Ultra-Weak Photon Emission in Plants

Responsible Author for Material Distribution:

The author responsible for distribution of materials integral to the findings presented in this article in accordance with the policy described in the Instructions for Authors (<https://academic.oup.com/plphys/pages/General-Instructions>) is Qing Zhao.

Abstract

Ultra-weak photon emission (UPE) is a noninvasive diagnostic tool that effectively reflects the function and health status of plant cells. However, current UPE measurement techniques are limited by resolution and sensitivity, particularly when monitoring different plant species and stress types. This study analyzes the delayed luminescence (DL) properties of *Hydrocotyle vulgaris*, *Arabidopsis* leaves, and *Ginkgo* leaves under both stress and control conditions using an independently developed UPE imaging system. The results showed a significant increase in initial DL intensity and an accelerated oxidative metabolic rate under mechanical injury and oxidative stress. DL decay characteristics were significantly correlated with the plant's physiological state, with stress conditions exhibiting decay curves that closely matched theoretical models. These findings confirm the established correlation between DL and plant stress responses. The high-resolution, low-noise imaging system significantly improves the accuracy of plant physiological state monitoring and provides new insights into the potential of optical signals for non-chemical communication research and agricultural applications. This technology has great potential for monitoring plant growth, assessing environmental stress, and supporting precision agriculture.

Keywords ultra-weak photon emission, delayed luminescence, oxidative stress, reactive oxygen species, plant stress monitoring

Introduction

Ultra-weak photon emission (UPE), an inherent property of all living systems, has been observed across a diverse range of organisms, including animals, plants, and microorganisms. It is defined as the spontaneous emission of a weak photon stream by organisms during metabolic processes. The intensity of this emission typically ranges from a few photons to a few hundred per square centimeter and wavelengths between 180–800 nm. This emission can be considered a reflection of the organism's local energy state^[1].

In eukaryotic cells, the primary sources of UPE are the excited-state carbonyl ($^3R=O\cdot$) or singlet oxygen (1O_2) generated during oxidation, which serves as the ultimate photon emitters. The mechanism of their formation is well known^[2]. During normal oxidative

metabolism, organisms produce small amounts of reactive oxygen species (ROS), which are essential precursors of UPE. NADPH oxidase is a multi-subunit membrane protein complex typically found in cellular membranes, including the inner membranes of mitochondria and chloroplasts. The enzyme acts as an electron donor and facilitates the electron transfer reaction between a substrate and molecular oxygen (O_2), thus forming the superoxide anion (O_2^-). Subsequently, the action of enzymes, such as superoxide dismutase, facilitates the rapid conversion of O_2^- into hydrogen peroxide (H_2O_2). H_2O_2 can undergo further reactions to produce the highly reactive hydroxyl radical ($HO\cdot$). $HO\cdot$ then reacts with proteins, lipids, nucleic acids, and other biomolecules in organisms to form alkyl radicals ($R\cdot$) [3], which subsequently combine with O_2 to form organic peroxy radicals ($ROO\cdot$). $ROO\cdot$ then reacts with other organic substances to form organic peroxides ($ROOH$) and $R\cdot$. The cyclization or recombination of $ROO\cdot$ can produce unstable, energetic intermediates, such as dioxetane ($ROOR$) and tetroxide ($ROOOOR$) [4-5]. These unstable intermediates decompose into triplet-excited carbonyls ($^3R=O\cdot$) and ground state carbonyls ($R=O$). The energy transfer from $^3R=O\cdot$ to pigments or O_2 results in the formation of the excited-state pigments ($^3P\cdot$ or $^1P\cdot$) and 1O_2 . These excited states release excess energy in the form of photons when they return to a lower energy state [6]. The energy of the photons emitted by various radiators corresponds to certain wavelength ranges in the electromagnetic spectrum. The emission wavelengths of $^3R=O\cdot$ are between 350–550 nm, while those of the pigments are between 550–750 nm ($^1P\cdot$) and 750–1000 nm ($^3P\cdot$). A simplified diagram of the above reaction mechanism is presented in Figure 1.

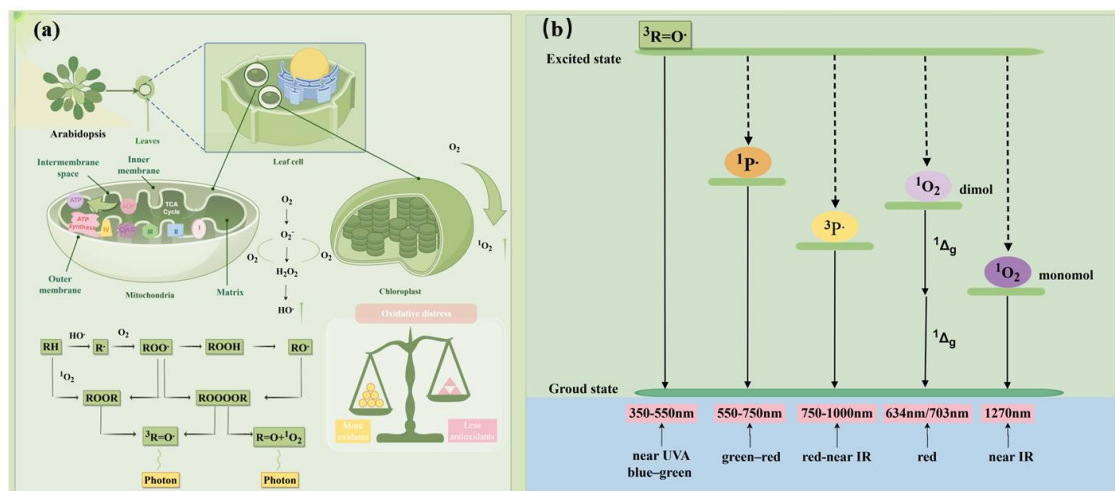


Figure 1. (a) Schematic representation of the UPE mechanism. NADPH oxidase is located within the

mitochondrial or chloroplast membranes, where it catalyzes the reaction between a substrate and molecular oxygen, resulting in the production of the O_2^- , which is subsequently converted to H_2O_2 and $HO\cdot$. $HO\cdot$ can then oxidize biomolecules. These unstable intermediates have high energy levels, as exemplified by ROOR and ROOOOR. They decompose into $^3R=O\cdot$ and $R=O$. $^3R=O\cdot$ then transfers energy to pigments or O_2 leading to the production of excited-state pigments ($^3P\cdot$ or $^1P\cdot$) and 1O_2 . The reaction scheme is based on^[2]. (b) UPE electronically excited species. $^3R=O\cdot$ emission wavelengths are located in the near-ultraviolet and blue-green regions, while the excited state pigments are located in the green-red ($^1P\cdot$) and near-infrared ($^3P\cdot$) regions. 1O_2 is in the red and near-infrared regions. The solid arrows indicate the energy level transitions from the excited state to the ground state, while the dashed arrows indicate the $^3R=O\cdot$ transitions and the energy transfer between the pigments and O_2 .

ROS concentrations during plant growth and metabolism are closely associated with UPE. Low ROS levels signal external stimuli, regulate plant growth and development, and work in synergy with other defense mechanisms to enhance plant resistance^[7]. However, when ROS levels remain persistently elevated, an oxidative stress response is triggered, impairing the plant's antioxidant system and causing oxidative damage to tissues^[8]. ROS accumulation disrupts the balance between production and scavenging, resulting in increased UPE intensity. The existing literature indicates that different stress conditions significantly affect plant UPE in varying ways. For example, in Arabidopsis, UPE increases and persists for several hours after mechanical damage, accompanied by changes in the spectral pattern of photon emission^[9]. The endogenous photon emission intensity of Arabidopsis seeds significantly increases during the early stages of seed germination, and this increase depends on the dose of locally applied H_2O_2 ^[10]. In sunflower plants subjected to biotic and abiotic stresses, a significant decrease in photon emission was observed in healthy plants under controlled growth conditions. In contrast, a marked increase was observed in stressed plants under water stress^[11]. Peanut and rice seedlings exhibited the most pronounced UPE when exposed to white light, followed by red and yellow lights. Conversely, the lowest luminescence intensity was observed under blue light. Under natural light conditions, UPE exhibited the slowest decay, while all other monochromatic lights exhibited faster decay rates than that of natural light^[12]. These results indicate that UPE, as a macroscopic manifestation of microscopic life activities, is highly sensitive to internal changes in plants and external

factors. Compared to traditional destructive detection methods (e.g., analysis of physiological and biochemical indicators), UPE is a noninvasive diagnostic tool that can be used to assess the physiological status of plants.

UPE can be divided into two main categories: spontaneous luminescence and exogenously induced luminescence. In the latter category, light-induced UPE is referred to as delayed luminescence (DL). DL refers to the emission of weak light radiation following the transition of a biological sample from a photoexcited state to a ground state after irradiation with white or monochromatic light. Compared to spontaneous luminescence, DL has a higher signal-to-noise ratio and luminescence intensity, with peaks reaching hundreds of thousands of photons per square centimeter. The DL phenomenon is closely related to various fundamental biological processes, including metabolic activities, growth and development, genetic variation, and intercellular information transfer. Consequently, it is a crucial and sensitive physical indicator for assessing the functionality and health status of biological cells^[13-19]. DL is closely associated with the excitation of coherent electron and exciton states in biological macromolecules, a conclusion that is supported by experimental evidence^[20-22]. The advantages of DL—high sensitivity, convenient operation, rapid response, and nondestructive detection—have led to its widespread use in various fields. These fields include the differentiation of normal cells from tumor cells^[23], the determination of seed germination^[24,25], the identification of herbal medicines^[26-29], food safety assessment^[30], and fruit ripening^[31]. The results of these studies demonstrate that changes in DL parameters can effectively reflect the physiological state of organisms, thus providing new insights and avenues for the advancement of bioanalytical techniques based on changes in DL. Despite some progress in the study of DL in plants, the field still presents significant challenges. Current techniques do not overcome the problems of weak plant DL signals, interference from background noise, and variability across different plant species and environmental conditions. Additionally, the underlying mechanism of DL remains poorly understood, and the relationship between light signal attenuation and physiological changes in plants in response to environmental stress has not been fully elucidated. There is considerable scope for improving the existing technology, particularly in terms of imaging resolution, signal sensitivity, and data processing accuracy.

In light of the above considerations, this study proposes the implementation of a light-induced methodology for the systematic observation of DL in *Hydrocotyle vulgaris*, *Arabidopsis* and *Ginkgo* leaves under natural growth conditions, considering different stress factors. The methodology involves using a highly sensitive two-dimensional photon imaging technique, which enables effective monitoring of oxidative metabolic processes in plants and their responses to oxidative stress. Additionally, a comprehensive investigation of the DL decay kinetics in plant leaves will be conducted to elucidate the relationship between changes in DL parameters and plant physiological states. This study aims to provide a new basis for understanding the quantum effects and the physical mechanisms of UPE.

Results

DL of three plant species in their natural state

Arabidopsis plants and leaves, *H. vulgaris* leaves, and *Ginkgo* leaves were imaged in their natural state, as shown in **Figure 2(a)**. **Figure 2(b)** presents the trend of DL intensity over time. After multiple exposures, the DL intensity of all three plants exhibited a nonlinear decay trend, characterized by an initial high intensity followed by a rapid decline and subsequent stabilization. This observation suggests that by the end of the measurement period, the plants' DL had almost ceased and had entered a stable spontaneous luminescence phase.

The DL decay differed significantly between the *Arabidopsis* plant and its leaves. The plant had a higher initial intensity (0.2736) than the leaves (0.2258) and stabilized earlier. In contrast, the leaves showed greater fluctuation, with a notable decrease at $t = 120$ s, slight recovery, and then stabilization, reflecting different metabolic and physiological responses.

The DL ability also varied between plant species. *Arabidopsis* leaves had the weakest and shortest luminescence, with a rapid decay. *H. vulgaris* had a higher initial intensity (0.3037) but decayed quickly, with a brief luminescence duration. *Ginkgo* leaves had the strongest and most persistent delayed luminescence, with the highest initial intensity (0.5353) and a slower decay rate, maintaining a high intensity for a longer period.

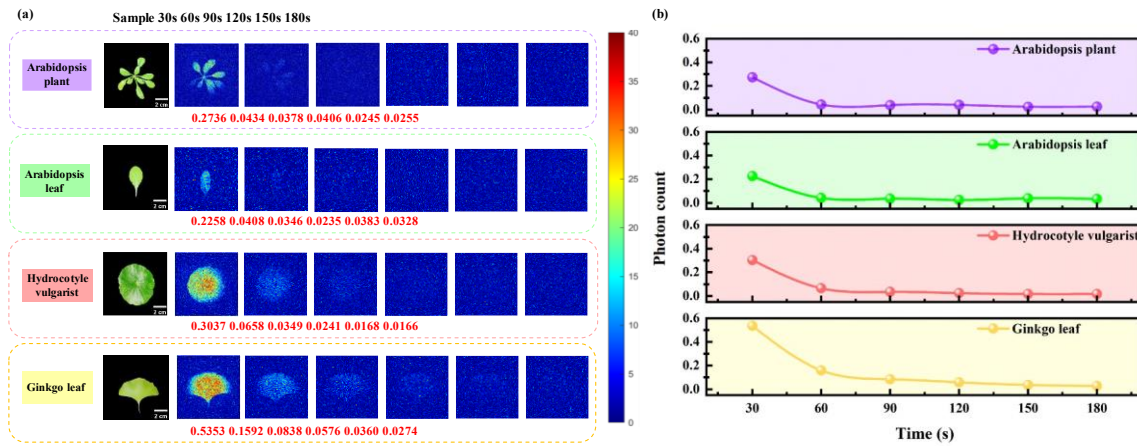


Figure 2. (a) DL imaging results of Arabidopsis (plants and leaves), *H. vulgaris* leaves, and Ginkgo leaves in the natural state. Sample sizes are presented in front of the qCMOS camera. The exposure time was 30 s, and the total measurement time was 180 seconds. The red data represents the DL intensity. The image size was 230×230 pixels. Subsequent figures follow a similar pattern. (b) The trend of DL intensity over time.

DL of three plant species under stress

Effects of mechanical injury

The DL Imaging System monitored the changes in DL intensity of *H. vulgaris*, Arabidopsis, and Ginkgo leaves after mechanical injury. **Figure 3(a)** illustrates the imaging results of leaves from the three plants under control and injury conditions, with the red line denoting the injury site. The data for the first 30 seconds are shown in the figure, while the data for the first 90 seconds can be found in the **Supplementary Figure S1**. 3D waterfall plots of DL intensity and its decay for three plants at different injury times are shown in **Supplementary Figure S2**. **Figure 3(b)** presents a histogram of the difference in DL intensity between the mechanically injured group and the control groups over time, demonstrating the effect of mechanical injury on the DL. The fitting results (**Figure 3(c-e)**) indicated that the DL decay of *H. vulgaris* and Ginkgo leaves followed the exponential model (Eq.(5)) and Arabidopsis conformed to the polynomial model (Eq.(6)). The detailed regression coefficients (a), slope parameters (b), and fitting coefficients (R^2) are given in **Table 1** and **Table 2**, respectively.

In monitoring DL intensity imaging in different plants, we observed significant differences in their sensitivity and response time to mechanical injury. *H. vulgaris* showed a rapid and strong response within 5 min, with a marked increase in DL intensity to 0.6716, approximately 1.95 times that of the control group. Although the response diminished over time, it remained elevated, indicating a sensitive and prolonged response to mechanical injury. In contrast, *Arabidopsis* showed a more moderate response, with a smaller increase in DL intensity and less fluctuation, although the intensity gradually increased after injury. Ginkgo leaves showed a more stable response, with DL intensity increasing to 0.6693 within 5 min, approximately 1.56 times that of the control, and remaining at a high level for the remainder of the time period. These results highlight differences in the adaptive mechanisms of different plants in response to mechanical injury, with *H. vulgaris* and Ginkgo leaves showing more intense and sustained responses, whereas *Arabidopsis* showed relatively milder and less fluctuating responses.

The fitting results also indicated that the injury groups generally had higher initial intensities and faster decay rates, reflecting the rapid response mechanism that plants employ following mechanical damage. The R^2 values for all groups were close to 1, indicating an excellent model fit. Notably, the injury group exhibited a DL decay pattern that was highly consistent with the fitted model, indicating that the response of plants to mechanical injury follows a predictable pattern. In *Arabidopsis*, the injury group had a larger coefficient for the quadratic term, suggesting that its nonlinear decay component was more pronounced. The higher-order terms (A_3 and A_4) were negative in both the control and injury groups, with larger absolute values in the injury group, indicating greater volatility and more substantial decay in the higher stages of decay. In summary, the injury groups of all three plants showed greater consistency in initial intensity, decay rate, and model fit, underscoring the significant influence of mechanical injury on the DL decay pattern in plants.

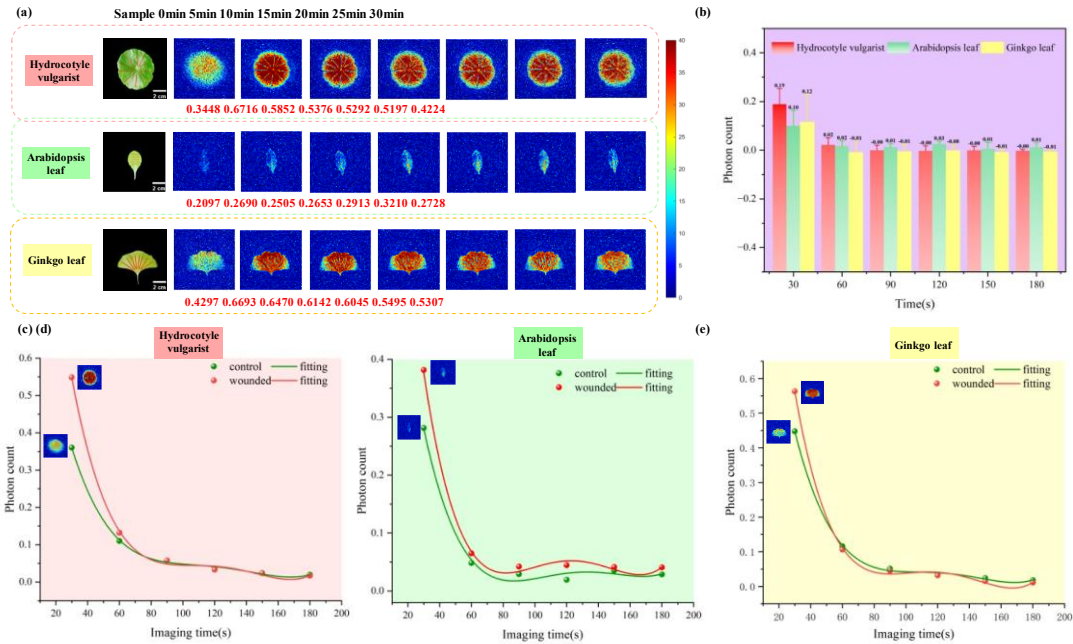


Figure 3. Effect of mechanical injury on plant DL. (a) Initial intensity ($t = 30$ s) imaging results of DL after mechanical injury in three plants. 0 min indicates the control. Time represents the duration of mechanical injury, which was monitored every 5 min for 30 min. Samples present the true state of the leaves before the experiment, with the red line indicating the location of the mechanical injury. (b) D-value in DL intensity in the stress and control groups. The error bar comes from the average of three measurements. (c-e) Examples of the fit of DL control and stress groups decaying over time for *H. vulgaris*, *Arabidopsis*, and *Ginkgo* leaves. The data comes from the average of three measurements.

Effects of oxidative stress

The leaves of *H. vulgaris*, *Arabidopsis*, and *Ginkgo* were treated with a 3% H_2O_2 solution, and the response was monitored using a DL imaging system. The resulting images are presented in **Figure 4(a)**, with 0 min representing the untreated control. Data for the first 30 seconds are shown in the figure, while the data for the first 90 seconds can be found in the **Supplementary Figure S3**. 3D waterfall plots of DL intensity and its decay for three plants at different oxidative stress times are shown in **Supplementary Figure S4**. Bar graphs were constructed to demonstrate the changes in DL intensity between the oxidative stress group and the control group (**Figure 4(b)**). **Figure 4(c-e)** presents the fitting of the intensity decay for the three plants during DL. The detailed regression coefficients (a), slope parameters (b), and

fitting coefficients (R^2) are given in **Supplementary Table 1** and **Supplementary Table 2**, respectively.

Monitoring and imaging the initial DL intensity of the three plants' leaves under oxidative stress over time revealed that different plants exhibited different response mechanisms. During the initial 5 min, the DL intensity of *H. vulgaris* decreased by 13.0% compared to the control group. However, after 30 min, it returned to a higher level, indicating a robust antioxidant capacity. *Arabidopsis* displayed a more sensitive response to oxidative stress, with a sustained decrease in DL intensity. At the 5-minute mark, its DL intensity decreased to 0.2375, representing a 24.3% reduction. Subsequently, the DL intensity decreased further to 0.2486 after 30 min, representing a total change of 27.4%. In contrast, the Ginkgo leaves displayed a remarkable ability to adapt to oxidative stress. Within the first 5 min, the DL intensity increased from 0.4555 to 0.4979, a change of 9.3%. After 30 min, the DL intensity continued to increase and reached 0.6546, an increase of 43.7%. These results indicate that the Ginkgo leaves could rapidly activate their antioxidant response mechanism, resulting in increased DL intensity. The results revealed that the three plants had different response mechanisms when exposed to oxidative stress, and applying H_2O_2 facilitated changes in the DL intensity of the plants.

Data fitting results indicated that the decay of DL in the three plants under oxidative stress was more consistent with the fitted model, suggesting that oxidative stress had a significant impact on the plants' DL characteristics. Oxidative stress significantly increased the initial DL intensity in both *H. vulgaris* and Ginkgo leaves, with Ginkgo leaves exhibiting an initial intensity nearly three times higher than that of the control group, indicating a stronger response to oxidative stress. Regarding the decay rate, *H. vulgaris* showed a slight increase with no significant change, while Ginkgo leaves showed a significantly faster decay rate, reflecting their stronger adaptive capacity. In contrast, *Arabidopsis* showed a faster decay rate, indicating a weaker ability to cope with oxidative stress. These results highlight the different response mechanisms of the three plants under oxidative stress and underline the high sensitivity of DL imaging as an effective tool for monitoring oxidative responses in plants.

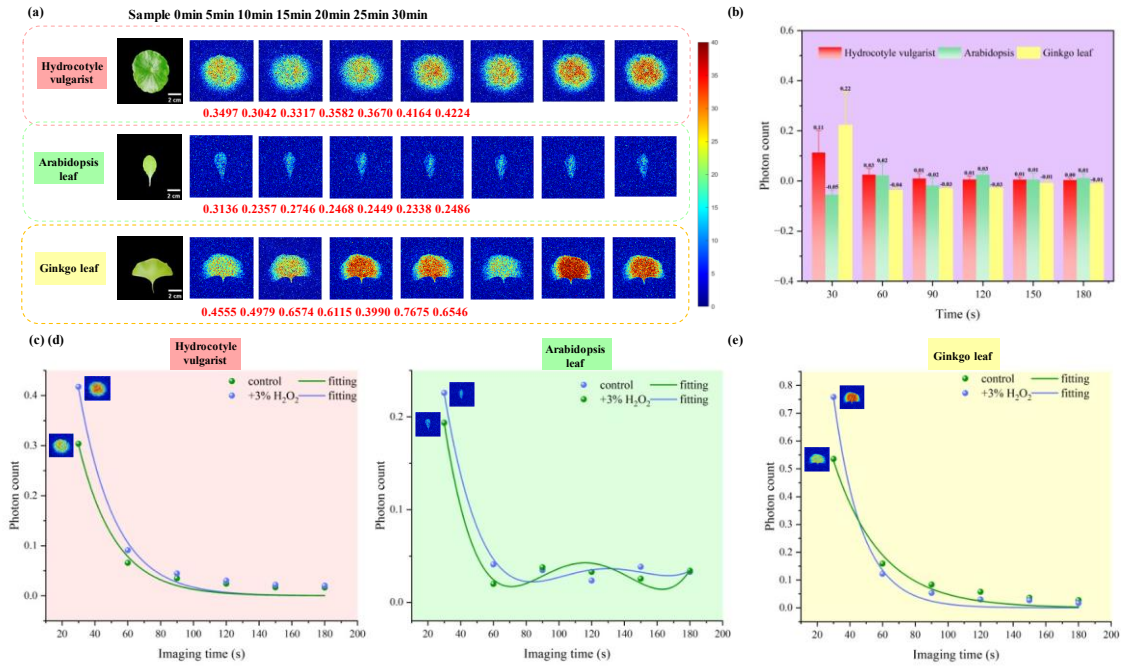


Figure 4. Effect of oxidative stress on plant DL. (a) Initial intensity ($t = 30$ s) imaging results of DL after oxidative stress in three plants. 0 min indicates the control. Time represents the duration of oxidative stress, which was monitored every 5 min for 30 min. Samples present the true state of the leaves before the experiment. (b) D-value in DL intensity in the stress and control groups. The error bar comes from the average of three measurements. (c-e) Examples of the fit of DL control and stress groups decaying over time for *H. vulgaris*, *Arabidopsis*, and *Ginkgo* leaves. The data comes from the average of three measurements.

Effect of different light qualities

Figure 5(a) presents the results of the DL imaging of plant leaves under white, red, and blue lights. **Figure 5(b)** and **Figure 5(c)** compare the effects of different light qualities on the DL of the same plant and an analysis of the DL intensity of the three plants under different light qualities at the same exposure time. **Figure 5(d-f)** presents an example of the fitting of the DL decay with time for the three plants. The fitting results demonstrate that the decay patterns of *H. vulgaris* and *Ginkgo* leaves were consistent with the exponential model (Eq. (5)), whereas that of *Arabidopsis* displayed a polynomial decay pattern (Eq. (6)). The detailed regression coefficients (a), slope parameters (b), and fit coefficients (R^2) are presented in **Supplementary Table 3** and **Supplementary Table 4**.

Different light qualities significantly influenced the initial intensity and decay rate of DL in the leaves of the three plant species, with both common patterns and individual differences in their responses. Under white light, the initial luminescence intensity was highest and the decay rate was slow for all three plants. In contrast, under blue light, the intensity was the lowest and the decay rate was the fastest, particularly in *H. vulgaris* and Ginkgo leaves. Under red light, the DL intensity fell between that of white and blue light, and the decay rate was more moderate. These findings suggest that plant responses to different wavelengths of light vary significantly, particularly under white light conditions.

The observed differences among plants' responses were related to their photoacclimation mechanisms. Under white light, Ginkgo leaves exhibited the highest initial luminescence intensity, followed by *H. vulgaris*, with *Arabidopsis* showing the lowest intensity. The initial intensity of *H. vulgaris* was similar to and significantly higher than, that under blue light in both white and red light conditions, with DL persistence being significantly higher, especially under red light. In contrast, the luminescence intensity and decay rate of *Arabidopsis* showed less variation, particularly under red and blue light, and its response was more consistent. Under blue light, the R^2 value for *Arabidopsis* was 0.9998, indicating that its DL decay followed a polynomial model. Under red light, Ginkgo leaves displayed a higher initial DL intensity and a slower decay, exhibiting an exponential decay pattern similar to that of *H. vulgaris*.

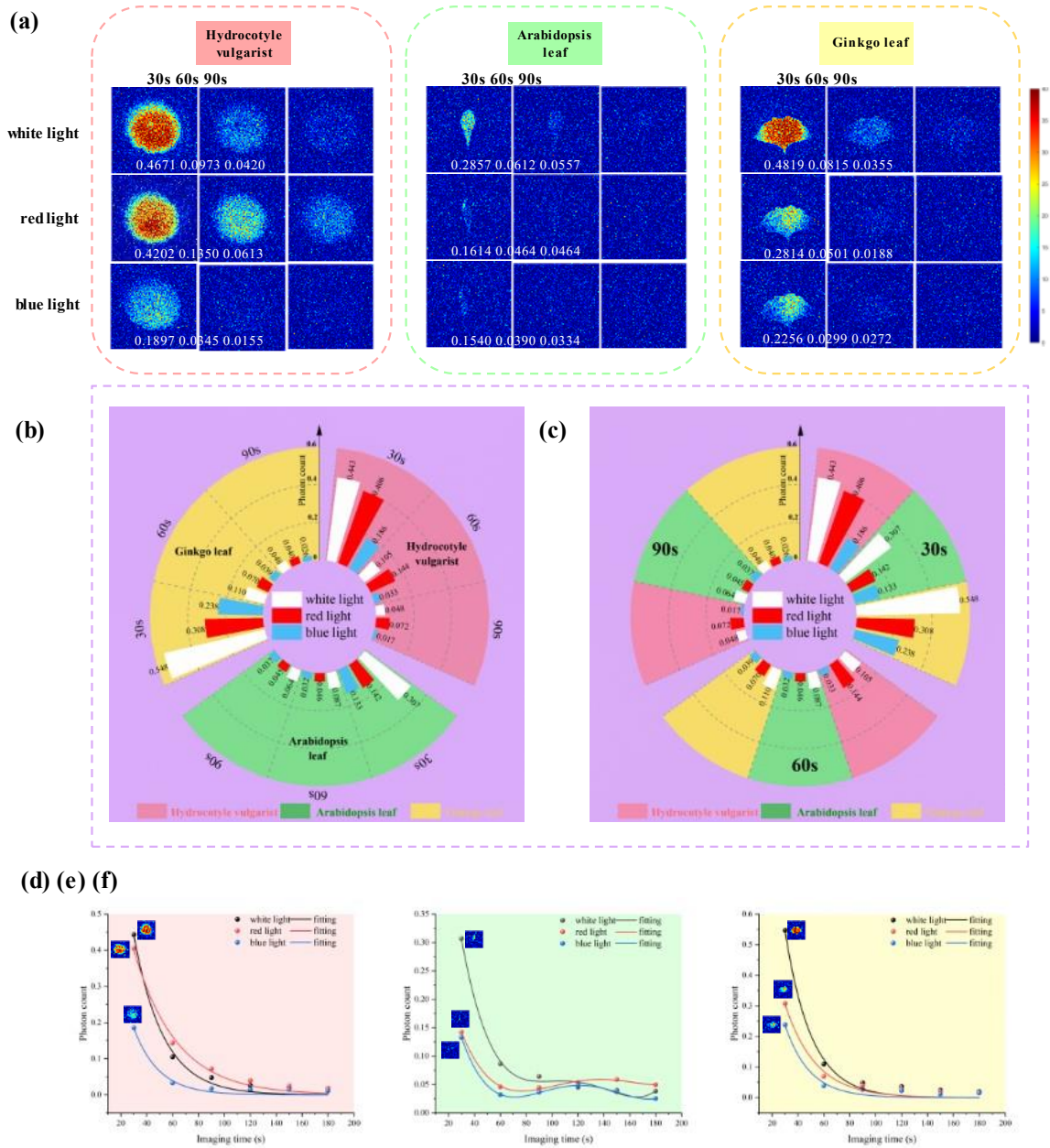


Figure 5. The effect of different light qualities on plants' DL. (a) DL imaging results of the three plants under white, red, and blue light irradiation presented for a single measurement with an exposure of 30 s, for a total of 180 s. The results for the first 90 s are presented. (b) Decreasing trend of DL with increasing exposure time for the same plant under different light qualities. (c) Decreasing trend of DL intensity of three plants with the same exposure time under different light qualities. (d-f) Fitted curves of DL decay with time for *H. vulgaris*, *Arabidopsis*, and *Ginkgo* leaves under different light qualities. The data represent the mean of three measurements.

Physical mechanisms and quantum modeling of DL in plants

The observed DL in plants and the luminescence process of glow sticks have similarities. Specifically, the luminescence mechanism of glow sticks comprises a series of chemical reactions triggered by physical stimuli (e.g., bending). In this process, H_2O_2 inside the glow stick reacts with the fluorescent dye, decomposing and producing water and high-energy $^1\text{O}_2$. The $^1\text{O}_2$ then exchanges energy with the fluorescent dye, causing the dye molecule to jump to the excited state. When the dye molecule returns to its ground state, energy is released in the form of photons, producing visible light. This luminescence mechanism is analogous to the DL phenomenon in plants, particularly in chemical reactions involving H_2O_2 .

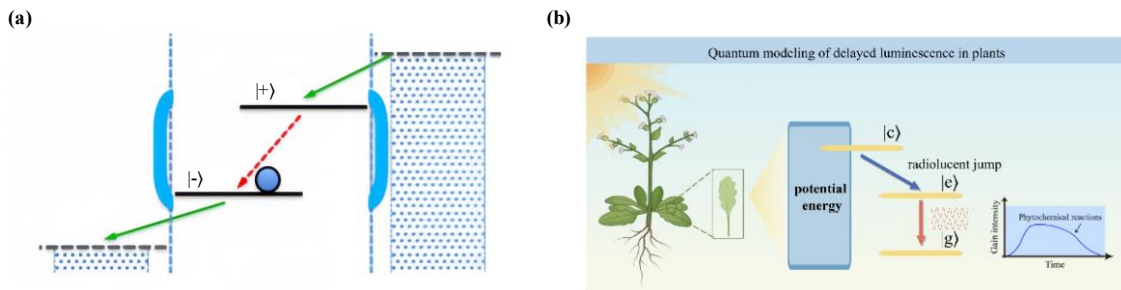


Figure 6. Physical mechanisms and quantum modeling of DL in plants. (a) Theoretical model of quantum dot luminescence. The left and right sides indicate two electrodes, and the top line indicates the electrochemical potential of the two electrodes. (b) Theoretical model of DL in plants. e and g denote the two energy levels of the final luminescence, and the left side denotes the chemical potential provided by the complex chemical reaction process. The graph represents the trend of the gain intensity with the course of the chemical reaction.

To further quantify the plant luminescence process, we borrowed the model of quantum dot luminescence to describe its luminescence mechanism. **Figure 6(a)** illustrates the luminescence process of quantum dots, in which electrons jump from the electrodes to the upper energy level of the quantum dots and from the upper energy level to the lower energy level, emitting photons in the process. The energy of the luminescence process comes from the “electrochemical potential” of the electrons in the electrode. The DL of plants, Conversely, is an energy transfer process driven by the chemical potential provided by a chemical reaction. Therefore, there exists a similarity in the nature of the energy transfer between the two phenomena.

The process of plant luminescence is triggered by a complex chemical reaction (**Figure**

6(b)). In this process, the jump between the excited state and the ground state determines the final luminescence intensity. Assuming that the electron jumps in the process of plant luminescence follow an energy transfer mechanism similar to that of quantum dot luminescence, we can simplify it into two energy levels: the ground state (g) and the excited state (e). A chemical reaction causes the electrons in the excited state to occupy the number N_e , which decreases with the decay term, providing sufficient chemical potential and releasing energy to produce light, as per the following equation:

$$\partial_t N_e = -\gamma N_e + \kappa N_c \quad (1)$$

$$\partial_t N_c = -\Gamma_t^- N_c + \Gamma_t^+ N_g \quad (2)$$

Eq. (1) describes the excited state generation process, where the first term represents the decay of the occupation number N_e of the excited state with time and is the rate constant for the jump from the excited state (e) to the ground state (g). The second term represents the increase in N_e due to the transition from the intermediate state (c) to the excited state (e) and is the rate constant for the jump. Eq. (2) describes the evolution of the occupancy number N_c of the intermediate state with time, where Γ_t^- is the rate constant for the transition from the intermediate state (c) to the excited state (e), and Γ_t^+ corresponds to the rate constant for a chemical reaction to excite an electron to a higher energy state. As a result of the chemical reaction, the system's energy changes from the lowest to a higher state. By analogy with the quantum dot luminescence process, we propose to write these two jump coefficients as $\Gamma_t^+ \equiv \gamma_0 \bar{n}_t$, $\Gamma_t^- \equiv \gamma_0 (1 - \bar{n}_t)$, where n_t denotes a quantity analogous to the chemical potential and varies with the chemical reaction process.

The model's predictions regarding the kinetics of the chemical reactions were effectively verified in the experiments. The experimental results revealed that mechanical injury and oxidative stress significantly increased the DL intensity of plants, a phenomenon consistent with the description of the electron jump rate and energy transfer in the model. Mechanical injury disrupted plant cellular structures and induced ROS accumulation. This process accelerated the electron jump from the excited state to the ground state and increased the DL intensity. Conversely, oxidative stress increased the luminescence intensity by increasing the H_2O_2 concentration, which increased the chemical potential of the reaction and the number of electrons occupying the excited state and facilitated the electron jump. In a

study of the effect of different light qualities on DL in plants, the photosynthesis efficiency was higher under white light irradiation. Compared with monochromatic light irradiation, white light activated stronger chemical reactions and promoted the conversion of electrons from the intermediate to the excited states. Additionally, white light irradiation may promote the production of photosynthetic intermediates (e.g., ATP and NADPH), which is directly related to the chemical potential provided by the chemical reactions in the model. According to the model, the metabolites provided additional energy for electron jumps under light irradiation, further facilitating the electron transfer from the excited state to the ground state and increasing the DL intensity. This result is consistent with the experimental observations, suggesting that the wavelength of the light source during photosynthesis directly affects the DL intensity and decay characteristics.

Furthermore, for the simplified two-energy system, we can derive the following evolution equations:

$$\partial_t N_e = -\gamma N_e + G(t)N_e \quad (3)$$

where $G(t)$ denotes the gain of the chemical reaction for N_e . Although these equations are time-inclusive, considering the slower rate of the chemical reaction relative to the luminescence process, we can assume that $G(t)$ changes gradually with time and stabilizes on longer time scales. In the solution of the model, we can approximate the process to obtain the N_e , the time evolution of the plant's luminescence: $N_e(t) \cong C \exp[\gamma t + G(t)t]$, and thus derive the decay properties of plant luminescence. Additionally, combining the polynomial and exponential decay terms, a functional model for fitting the DL data was built:

$$D(t) = \sum a_i t^i \cdot e^{-\gamma t} \quad (4)$$

where $D(t)$ is the luminous intensity, a_i is the polynomial coefficient, γ is the decay rate, and t is the time. The model can capture the time-dependent characteristics of the DL process in plants well, especially the decay trend on long-time scales.

Through the above model, we can further explore the quantitative features of the DL process, especially by analyzing the second-order autocorrelation function of DL, $g^{(2)}(t)$, to reveal the intrinsic law of the plant luminescence mechanism. Additionally, we can accurately characterize the temporal and spatial properties of the luminescence process in

plants by adjusting the parameters in the model, which can provide a theoretical basis for further studies on the effects of plant physiology and chemical reactions on the luminescence phenomenon.

Discussion

DL imaging is an emerging biomonitoring tool that offers higher sensitivity, rapid response, and noninvasive assessment of oxidative stress levels in plants compared with traditional biochemical and molecular assays. In this study, we systematically analyzed the DL properties of three plants under natural growth and stress-induced conditions. The results revealed that the DL intensity was significantly correlated with the stress level of the environment to which the plants were exposed. The physiological status of plants under different types of stress changed significantly, and these changes could be effectively monitored by the DL intensity fluctuations. In an environment of high oxidative stress, the plants displayed stronger DL intensity, reflecting their ability to respond to environmental stress. Additionally, by combining this tool with image pattern recognition and statistical analysis, we could accurately indicate the health status of plants, providing a new technological tool for future plant health monitoring and management. DL imaging enables us to assess and intervene in plant growth status in a timely manner before visual symptoms become apparent, thus improving the sustainability of agricultural production.

Measuring DL intensity under natural growing conditions provides a valuable basis for assessing plant health status and normal metabolic processes. Analyzing the decay pattern of DL intensity over time gave us insight into the oxidative metabolic state of plants and revealed the dynamic changes in intracellular ROS. These findings provide new perspectives for understanding the metabolic activities of plants under natural conditions.

Plants undergo oxidative metabolism and produce a certain amount of ROS during normal growth; however, when they are subjected to mechanical injury, ROS production increases significantly, leading to oxidative stress. In this case, the plant's antioxidant system cannot effectively scavenge the excess ROS, leading to their accumulation. This imbalance between generation and scavenging exacerbates oxidative stress, further damaging biomolecules like proteins, lipids, and nucleic acids in the leaves. At the same time, the ROS

accumulation may contribute to the production of more high-energy states in plant cells, which release more photons when jumping to the ground state. As a result, the initial DL intensity of the damaged group was usually higher than that of the control group.

The differences in the responses of different plants to mechanical injury reflect their different mechanisms of response to oxidative stress. Our results revealed that the DL intensity significantly increased in mechanically injured plants, which is consistent with the findings of Prasad et al^[9]. Additionally, *H. vulgaris* displayed a strong oxidative stress response, whereas *Arabidopsis* was more stable, and Ginkgo leaves responded significantly in terms of initial DL intensity but declined more significantly over time. Future studies could further explore how the DL property can enhance the stress tolerance performance of plants.

Endogenous metal ions in plants (e.g., Fe^{2+} or Cu^{2+}) react with exogenous H_2O_2 solutions in a Fenton reaction to produce $\text{HO}\cdot$, which accelerates oxidative reactions in plants^[2]. To test this hypothesis, we treated the leaves of three plants (*H. vulgaris*, *Arabidopsis*, and Ginkgo leaves) with a 3% H_2O_2 solution and monitored their responses using a DL imaging system. The results revealed that the initial DL intensity significantly increased in plants under oxidative stress. Exogenous H_2O_2 induced oxidative stress and reacted with intracellular metal ions to generate hydroxyl radicals and hydroxide ions, which increased the intracellular ROS concentration and significantly increased the DL intensity. However, with H_2O_2 depletion and the excited-state substances, the DL intensity gradually decreased and eventually tended toward the steady state. The differences in the responses of different plants to oxidative stress may be due to their differences in the rate of the Fenton reaction or the primary oxidation reaction, which directly affects the DL intensity and its decay time. Our results indicated that *H. vulgaris* and Ginkgo leaves could effectively regulate the intracellular ROS levels, resulting in an increase in DL intensity, whereas *Arabidopsis* exhibited higher sensitivity, resulting in a decrease in DL intensity. Related studies have also demonstrated the critical role of H_2O_2 and oxidative processes in UPE; for example, the UPE intensity in potato tubers was significantly correlated with endogenous H_2O_2 ^[32].

Photobiology is an essential field that studies the effects of light on plant physiology, development, and ecology. The health status of plants under different light qualities is usually assessed by indicators like the photosynthetic rate, respiration rate, and chlorophyll content.

Compared with static bioindicators, DL imaging provides more detailed dynamic information and can effectively integrate the complex relationship between light quality, time, and plant physiological status. The results revealed that the DL intensity in plants under white light was significantly higher than under red and blue lights, further confirming the importance of the light source wavelength in plant physiological responses. Different light qualities had different effects on the DL decay rate in plants: white light had the highest initial DL intensity and a slow decay rate, while blue light had the lowest initial DL intensity and fastest decay rate. Ginkgo leaves had the highest initial intensity in all experimental conditions, followed by *H. vulgaris*, while *Arabidopsis* had a relatively low DL intensity. Notably, the DL properties of *H. vulgaris* exhibited unique variations under red light conditions, suggesting a higher sensitivity to that wavelength. Related studies have demonstrated that different light wavelengths interact with each other through relevant pigments to affect the hormonal balance in plants, which in turn triggers physiological and ecological changes in plants^[33,34]. We hypothesize that the differences in the response mechanisms of plants under different light conditions may be due to their different internal pigment systems, which have different absorption and utilization capabilities for different light wavelengths, thus affecting plant growth and development.

Additionally, we analyzed the DL decay properties and verified the consistency of the quantum model with experimental data. By simplifying the theoretical DL model (Eq. (4)), several fitting forms were derived by combining different experimental data and limiting cases. By adjusting key parameters in the model (e.g., the decay rate γ), we investigated the main DL decay modes and the differences between plant species. The experimental data revealed that the DL intensity of *H. vulgaris* and Ginkgo leaves decayed exponentially with time, indicating that the DL of these plants is mainly driven by fast and direct processes, which is consistent with the assumption of an exponential decay term in the theoretical model. When the decay rate γ is negative (i.e., $\gamma = -b$, where b is a positive decay constant), the model exhibits an exponential decay property (Eq. (5)). The exponential decay term describes the rapid decrease in the luminescence intensity with time. However, the DL decay in *Arabidopsis* does not strictly follow the exponential decay law and displays a more complex time dependence. This deviation could be related to intermediate reactions, complex

molecular interactions, or multistep energy transfer processes. Therefore, the DL properties of Arabidopsis must be described by a more complex polynomial model, especially for longer decay times, where the polynomial part can better capture the complexity of the luminescence process. As the decay rate γ tends to zero, the exponential decay term $\exp(-\gamma t)$ becomes 1, and the model simplifies to the polynomial form presented in Eq. (6), at which point the luminescence intensity is no longer affected by the exponential decay and represents a purely polynomial process.

From a theoretical modeling perspective, exponential decay, which assumes that the system follows a single decay pathway, is more effective for the DL decay in *H. vulgaris* and Ginkgo leaves, but it is difficult to fully capture the complex interactions in biological processes. For example, the system may contain multiple reactants, different decay channels, or nonlinear interactions between molecules, which can lead to more complex decay properties, as observed in Arabidopsis. For all plant samples, the polynomial part of the theoretical model can, in some cases, better describe the complexity of the luminescence process.

Although the theoretical model better fits the DL process in the experimental data, it still has some limitations. For example, the model parameters depend on the experimental conditions and can be influenced by plant species, chemical reaction rates, and external environmental factors (e.g., temperature and light). Therefore, the parameters must be adjusted to improve the fitting accuracy under different experimental conditions. Future studies should consider more complex physical models that introduce higher-order decay functions and biological factors to improve the understanding of the DL process in plants further.

The present study reveals the differences in the oxidative metabolic capacity of different plants by comparing the DL characteristics of three plants. The results demonstrate that DL intensity and decay rate can effectively reflect the physiological status of plants. DL, as a sensitive physiological detection method, provides valuable information for understanding plant response mechanisms in complex environments. This finding provides a new perspective for the study of plant adaptation mechanisms to adversity and provides a scientific basis for future plant health monitoring and management.

Conclusion

Using a high-resolution and low-noise imaging system, this study provides a highly accurate noninvasive plant monitoring method that can effectively reflect plant cells' physiological status and health level. This method provides a new idea for the study of plant stress response and offers a wide range of application potentials, especially in plant health monitoring, environmental stress assessment, and precision agriculture management, with important practical significance. In the future, by combining DL technology with quantum physics modeling, we expect to further elucidate the response mechanism of plants to their external environment and provide new technical approaches and theoretical support for the realization of precision agriculture and the enhancement of plant resistance.

Material and Methods

Plant material and growing conditions

Hydrocotyle vulgaris is a perennial herbaceous wet plant of the genus *Hydrocotyle*. It is native to Europe, south North America, and Central America. Due to its rapid reproduction, large population, and strong adaptability, *H. vulgaris* is classified as an invasive plant in China^[35]. Our research team purchased *H. vulgaris* from the flower market of the Chinese Academy of Agricultural Sciences and grew it in a well-lit environment at a suitable room temperature. During the experiment, the plants were watered regularly to prevent wilting, and new leaves of similar age and size were selected for each measurement to ensure comparable data.

Arabidopsis thaliana is an annual herbaceous plant belonging to the Cruciferae family and is an important model organism in molecular genetics research. The Columbia ecotype (Columbia, Col-0) was used in this study. Seeds were soaked in distilled water at 4°C for 4 days before being planted in growing pots containing peat substrate (Klasmann, Potground H). *Arabidopsis* plants were grown under a 16-h light/8-h dark photoperiod with a photon flux density of $100 \mu\text{mol}\cdot\text{m}^{-2}\cdot\text{s}^{-1}$, with the ambient temperature maintained at 25°C and 60% relative humidity. The growth cycle was completed in 6–7 weeks. New plants or leaves of approximately the same age and size were selected for each measurement to ensure

consistency.

The Ginkgo tree is a perennial deciduous tree belonging to the genus *Ginkgo* in the family Ginkgoaceae. It is rich in various biologically active components, including flavonoids and pigments, which give it a high medicinal value. The leaves were harvested on the campus of the Beijing Institute of Technology, and the research team selected only healthy leaves free from pests and avoided picking fallen or discolored leaves to ensure the quality of the samples and the reliability of the experimental results.

DL imaging system

The configuration of the DL imaging system for radiation detection is presented in **Figure 7**. The system comprises four main components: a sample chamber, a qCMOS camera, a water-cooling system, and a computer. Due to the extremely low intensity of the DL photon flux emitted by the organism, a highly sensitive qCMOS camera (Hamamatsu ORCA-Quest) was selected. The camera's qCMOS imaging sensor has single photon sensitivity and subpixel readout noise characteristics, minimal dark current signal loss, and is equipped with a two-dimensional photon counting function that allows simultaneous acquisition of temporal and spatial information on DL intensity. The camera operates in the single photon number resolved mode with a scan rate of 17.6 frames per second and has a spectral sensitivity of 400–1000 nm with a quantum efficiency of up to 85%. The accompanying Computar objective (M2514-MP2, $f = 25$ mm) allows efficient DL measurement in organisms. A water-cooling system (LX-150 cooling circulator) was used to maintain the temperature of the camera at -40°C and minimize the occurrence of dark counts. The experiment was conducted in an opaque darkroom, with similarly sized intact plant samples (plants or leaves) positioned on a completely sealed black dark box sample stage, which was located within the camera's field of view. For each measurement, the same image acquisition parameters were maintained, with a single imaging exposure time of 30 seconds and six consecutive measurements with a cumulative imaging time of 180 seconds. The distance between the plant and the detector was 25 cm, and the distance between the leaf and the detector was 5 cm. After acquiring the detector signal, the data were transferred to a computer outside the darkroom. HCImage software was used for image acquisition and analysis, while

data correction was achieved by subtracting the background signal before each measurement. Image processing techniques were also integrated to improve the measurement system's image quality.

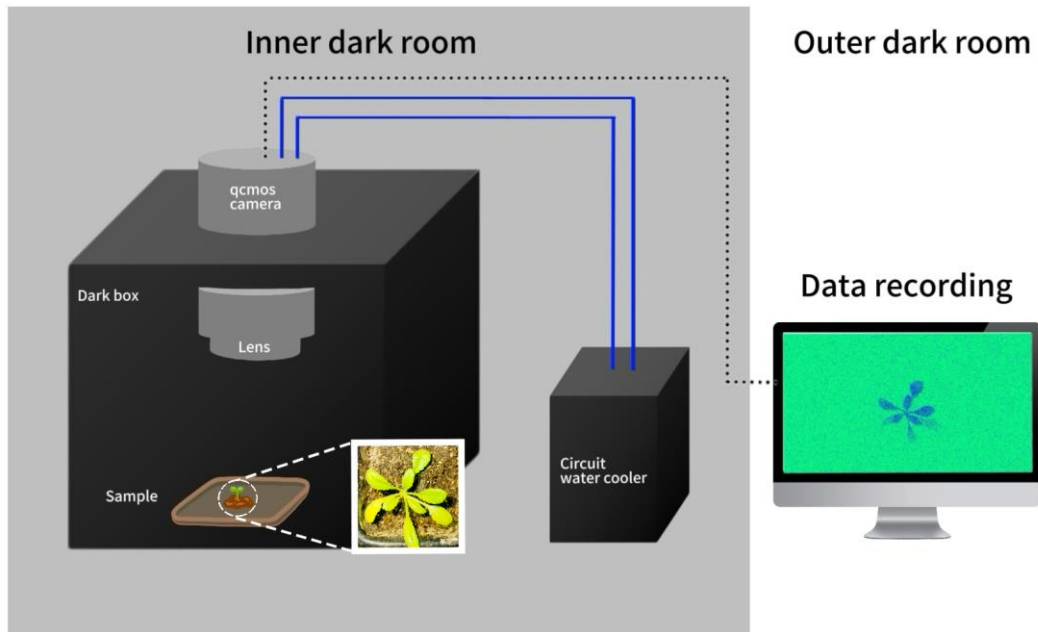


Figure 7. Schematic of DL imaging.

Experimental methods and stress treatments

The experiments were conducted in a dark room with the temperature maintained at 18°C. The air conditioning was run for 1 h before the start of the experiment, and the apparatus was allowed to reach equilibrium for 30 min to ensure the stability of the background signal and consistency of the ambient temperature. All biological samples were allowed to acclimatize in an external dark room for 30 min before measurement to minimize the effects of the environment and prevent the material's residual luminescence from affecting the results. Measurements were made by illuminating the sample and measuring the intensity of photons re-emitted from the sample after the light source was switched off. Because different leaf areas were used for each sample, the DL intensity was normalized to the photon intensity emitted per unit time and per unit leaf area. During the measurement process, fresh leaves of comparable growth stage were selected. They were first washed with deionized water, and the surface moisture was removed with filter paper. The leaves were then exposed to a 220 V and 10 W white LED light source for 5 min. Then, they were quickly

transferred to the sample chamber, where measurements of the leaves' DL intensity decay over time immediately started. The total duration of each measurement was set at 180 s, with three consecutive measurements. Background noise measurements were conducted under the same experimental conditions to obtain the final DL intensity measurements. These values were then subtracted from the average of the three measurements to obtain the final result.

Mechanical injury

The plant leaves were mechanically damaged using a sharp blade in a low-light environment. Precautions were taken to avoid additional stress or damage to other parts of the plant samples. After 5 min of mechanical damage, the samples were exposed to a 220 V and 10 W white LED light source for 5 min. This step ensured that the leaves could quickly adapt to the changed environment. Following the illumination period, DL intensity measurements were initiated.

H₂O₂ processing

During the H₂O₂ treatment, a freshly prepared 3% H₂O₂ solution was applied evenly to the surface of the plant samples to ensure optimum leaf infiltration. An equal amount of water was used as a control treatment to ensure the reliability of the experimental results. After 5 min of H₂O₂ treatment, the samples were irradiated for 5 min under a 220 V and 10 W white LED light source. This step was done to promote the recovery of photosynthesis and related physiological responses. At the end of the treatment, DL measurements were started to assess the effect of H₂O₂ on the plants' DL.

Light quality

LED curing lights (emitting white, red, and blue) of 220 V and 5 W were used as different light sources. The white light source emitted a full spectrum of light, while the red and blue light sources had central wavelengths of 660 and 460 nm, respectively. During the experiment, plant leaves treated with deionized water were exposed to their respective light sources at 5 cm from the LED lamps for 5 min. After irradiation, the sample leaves were immediately transferred to the sample chamber, and their DL intensity measurement started immediately.

Curve-fitting model

A suitable mathematical model was selected to describe the DL decay curves and make a quantitative comparison of the differences in DL intensities exhibited by different plants. The DL intensity data (in counts per 30 s) of *H. vulgaris* and Ginkgo leaves over time were subjected to an exponential regression model as follows:

$$y = a \times \exp(b \times x) \quad (5)$$

where y is the response variable, x is the predictor variable, a is the regression coefficient representing the initial DL intensity, and b is the dynamic parameter of the exponential decay (i.e., the slope parameter) representing the DL decay rate.

For the *Arabidopsis* DL intensity data, a polynomial model was fitted with the following model form:

$$y = A_0 + A_1x + A_2x^2 + A_3x^3 + A_4x^4 \quad (6)$$

where y is the response variable, x is the predictor variable, and the DL is characterized by the parameters A_0 , A_1 , A_2 , A_3 , and A_4 .

Supplementary Data

Supplementary Figure S1. The dynamics of DL intensity for three plants (during the first 90 s) at different mechanical injury times.

Supplementary Figure S2. 3D waterfall plots of DL intensity and its decay for three plants at different mechanical injury times.

Supplementary Figure S3. The dynamics of DL intensity for three plants (during the first 90 s) at different oxidative stress times.

Supplementary Figure S4. 3D waterfall plots of DL intensity and its decay for three plants at different oxidative stress times.

Supplementary Table 1. Exponential model fit data for the effect of oxidative stress on DL in plants.

Supplementary Table 2. Polynomial model fit data for the effect of oxidative stress on DL in *Arabidopsis*.

Supplementary Table 3. Exponential model fitting data for the effect of different light

qualities on the DL in plants.

Supplementary Table 4. Polynomial model fit data for the effect of different light qualities on the DL in Arabidopsis.

Acknowledgments and Funding

This research did not receive any specific grant from funding agencies in the public, commercial, or not-for-profit sectors. Thanks to Figdraw (www.figdraw.com) for help with character cartoons.

Author Contributions

Yan-Xia Liu: Conceptualization, Methodology, Software, Investigation, Formal Analysis, Validation, Writing—original draft. **Hai-Yu Fan:** Methodology, Investigation, Formal Analysis. **Yu-Hao Wang:** Software, Data curation. **Yan-Liang Wang:** Conceptualization, Methodology. **Sheng-Wen Li:** Conceptualization, Methodology, Investigation. **Shi-Jian Li:** Conceptualization, Methodology, Writing—review & editing. **Xu-Ri Yao:** Conceptualization, Formal analysis, Methodology, Resources, Writing—review & editing. **Qing Zhao:** Resources, Supervision, Writing—review & editing.

Conflicts of Interest: The author declares no conflict of interest.

Table 1. Exponential model fit data for the effect of mechanical injury on DL in plants.

Plant species	control	wounded	control	wounded	control	wounded
	a	a	b	b	R ²	R ²
H. vulgaris	0.9704	2.0064	−0.0335	−0.0434	0.9826	0.9918
Ginkgo	1.5059	2.6518	−0.0406	−0.0517	0.9885	0.9933

Table 2. Polynomial model fit data for the effect of mechanical injury in Arabidopsis.

Arabidopsis	A ₀	A ₁	A ₂	A ₃	A ₄	R ²
Control	0.9158	−0.0311	3.8873E-4	−2.0743E-6	4.0124E-9	0.9937
Wounded	1.3328	−0.0476	6.2758E-4	−3.5203E-6	7.1168E-9	0.9983

References:

- [1] Slawinski J, Popp F-A. (1987) Temperature hysteresis of low level luminescence from plants and its thermodynamical analysis. *Journal of Plant Physiology*, 130 (2): 111-123. [https://doi.org/10.1016/S0176-1617\(87\)80215-8](https://doi.org/10.1016/S0176-1617(87)80215-8)
- [2] Pospíšil P, Prasad A, Rác M. (2014) Role of reactive oxygen species in ultra-weak photon emission in biological systems. *Journal of Photochemistry and Photobiology B: Biology*, 139: 11-23. <https://doi.org/10.1016/j.jphotobiol.2014.02.008>
- [3] Pospíšil P, Prasad A, Rác M. (2019) Mechanism of the formation of electronically excited species by oxidative metabolic processes: Role of reactive oxygen species. *Biomolecules*, 9(7): 258. <https://doi.org/10.3390/biom9070258>
- [4] Vacher M, Galvan I F, Ding B, et al. (2018) Chemi- and bioluminescence of cyclic peroxides. *Chemical Reviews*, 118(15): 6927-6974. <https://doi.org/10.1021/acs.chemrev.7b00649>
- [5] Miyamoto S, Martinez G R, Medeiros M H G, et al. (2014) Singlet molecular oxygen generated by biological hydroperoxides. *Journal of Photochemistry and Photobiology B: Biology*, 139: 24-33. <https://doi.org/10.1016/j.jphotobiol.2014.03.028>
- [6] Cifra M, Pospíšil P. (2014) Ultra-weak photon emission from biological samples: definition, mechanisms, properties, detection and applications. *Journal of Photochemistry and Photobiology B: Biology*, 139: 2-10. <https://doi.org/10.1016/j.jphotobiol.2014.02.009>
- [7] Neill S J, Desikan R, Clarke A, et al. (2002) Nitric oxide is a novel component of abscisic acid signaling in stomatal guard cells. *Plant Physiology*, 128(1): 13-16. <https://doi.org/10.1104/pp.128.1.13>
- [8] Mittler R, Vanderauwera S, Gollery M, et al. (2004) Reactive oxygen gene network of plants. *Trends in plant science*, 9(10): 490-498. <https://doi.org/10.1016/j.tplants.2004.08.009>
- [9] Prasad A, Gouripeddi P, Naidu Devireddy H R, et al. (2020) Spectral distribution of ultra-weak photon emission as a response to wounding in plants: an in vivo study. *Biology*, 9(139): 139. <https://doi.org/10.3390/biology9060139>

- [10] Saeidfirozeh H, Shafiekhani A, Cifra M, et al. (2018) Endogenous chemiluminescence from germinating *Arabidopsis Thaliana* seeds. *Scientific Reports*, 8(1): 16231. <https://doi.org/10.1038/s41598-018-34485-6>
- [11] Pónya Z, Somfalvi-Tóth K. (2022) Modelling biophoton emission kinetics based on the initial intensity value in *Helianthus annuus* plants exposed to different types of stress. *Scientific Reports*, 12(1): 2317. <https://doi.org/10.1038/s41598-022-06323-3>
- [12] Li D H, He Y H, Luo M Z, et al. (1998) Ultra-weak luminescence of peanut seedlings grown under different light qualities. *Biophysical Journal*, (3): 548-552.
- [13] Chwirot W B, Popp F A. (1991) White light induced luminescence and mitotic activity of yeast cells. *Folia Histochemica et Cytobiologica*, 29: 155.
- [14] Veselova T V, Veselovsky V A, Rubin A B, et al. (1985) Delayed luminescence of air-dry soybean seeds as a measure of their viability. *Physiologia Plantarum*, 65: 493-497. <https://doi.org/10.1111/1399-3054.ep12907483>
- [15] Veselova T V, Veselovsky V A, Kozar V I, et al. (1988) Delayed luminescence of soybean seeds during swelling and accelerated ageing. *Seed Science and Technology*, 16: 105-113.
- [16] Musumeci F, Triglia A, Grasso F, et al. (1994) Relation between delayed luminescence and functional state in soya seeds. *IL Nuovo Cimento D*, 16: 65-73. <https://doi.org/10.1007/BF02452003>
- [17] Musumeci F, Scordino A, Triglia A. (1997) Delayed luminescence from simple biological systems. *Rivista Di Biologia*, 90: 95-110.
- [18] Scordino A, Triglia A, Musumeci F, et al. (1996) Influence of the presence of atrazine in water on the in-vivo delayed luminescence of *Acetabularia acetabulum*. *Journal of Photochemistry and Photobiology B: Biology*, 32: 11-17. [https://doi.org/10.1016/1011-1344\(95\)07213-6](https://doi.org/10.1016/1011-1344(95)07213-6)
- [19] Popp F A, Li K H, Mei W P, et al. (1988) Physical aspects of biophotons, *Experientia*, 44: 576-585. <https://doi.org/10.1007/BF01953305>
- [20] Brizhik L, Musumeci F, Scordino A, et al. (2000) The soliton mechanism of the delayed luminescence of biological systems *Europhys. Epl*, 52: 238-44. <https://doi.org/10.1007/s10076-000-0000-0>

doi.org/10.1209/epl/i2000-00429-5

- [21]Brizhik L, Scordino A, Triglia A, et al. (2001) Delayed luminescence of biological systems arising from correlated many-soliton states. *Physical Review E*, 64: 031902. <https://doi.org/10.1103/PhysRevE.64.031902>
- [22]Brizhik L, Musumeci F, Scordino A, et al. (2003) Nonlinear dependence of the delayed luminescence yield on the intensity of irradiation in the framework of a correlated soliton model. *Physical Review E*, 67: 021902. <https://doi.org/10.1103/PhysRevE.67.021902>
- [23]Scordino A, Baran I, Gulino M, et al. (2014) Ultra-weak delayed luminescence in cancer research: a review of the results by the ARETUSA equipment. *Journal of Photochemistry and Photobiology B: Biology*, 139: 76-84. <https://doi.org/10.1016/j.jphotobiol.2014.03.027>
- [24]Costanzo E, Gulino M, Lanzanò L, et al. (2008) Single seed viability checked by delayed luminescence. *European Biophysics Journal*, 37: 235-238. <https://doi.org/10.1007/s00249-007-0221-8>
- [25]Grasso R, Gulino M, Giuffrida F, et al. (2018) Non-destructive evaluation of watermelon seeds germination by using delayed luminescence. *Journal of Photochemistry and Photobiology B: Biology*, 187: 126-130. <https://doi.org/10.1016/j.jphotobiol.2018.08.012>
- [26]Sun M, Li L, Wang M, et al. (2016) Effects of growth altitude on chemical constituents and delayed luminescence properties in medicinal rhubarb. *Journal of Photochemistry and Photobiology B: Biology*, 162: 24-33. <https://doi.org/10.1016/j.jphotobiol.2016.06.018>
- [27]Sun M, Chang W T, van Wijk E, et al. (2018) Application of delayed luminescence method on measuring of the processing of Chinese herbal materials. *Chinese Medicine*, 13(1): 43. <https://doi.org/10.1186/s13020-018-0202-0>
- [28]Sun M, Wang S, Jing Y, et al. (2019) Application of delayed luminescence measurements for the identification of herbal materials: A step toward rapid quality control. *Chinese Medicine*, 14(1): 47. <https://doi.org/10.1186/s13020-019-0269-2>
- [29]Jia Y, Sun M, Shi Y, et al. (2020) A comparative study of aged and contempor

- ary Chinese herbal materials by using delayed luminescence technique. Chinese Medicine, 15: 6. <https://doi.org/10.1186/s13020-020-0287-0>
- [30]Stolz P, Wohlers J, Mende G. (2019) Measuring delayed luminescence by FES to evaluate special quality aspects of food samples-an overview. Open Agriculture, 4(1): 410-417. <https://doi.org/10.1515/opag-2019-0039>
- [31]Triglia A, La Malfa G, Musumeci F, et al. (1998) Delayed luminescence as an indicator of tomato fruit quality. Journal of Food Science, 63(3): 512-515. <https://doi.org/10.1111/j.1365-2621.1998.tb15775.x>
- [32]Rastogi A, Pospíšil P. (2012) Production of hydrogen peroxide and hydroxyl radical in potato tuber during the necrotrophic phase of hemibiotrophic pathogen *Phytophthora infestans* infection. Journal of Photochemistry and Photobiology B: Biology, 117: 202-206. <https://doi.org/10.1016/j.jphotobiol.2012.10.001>
- [33]Li S M. (2000) Application of light quality control films in facility horticulture production. China Vegetable, (201): 56-59.
- [34]Zhao D L. (1995) Effect of light on seed dormancy and germination. Biological Bulletin, 30(8): 27-29.
- [35]Liu L, Alpert P, Dong B C, et al. (2017) Combined effects of soil heterogeneity, herbivory and detritivory on growth of the clonal plant *Hydrocotyle vulgaris*. Plant & Soil, 421(1): 429-437. <https://doi.org/10.1007/s11104-017-3476-6>